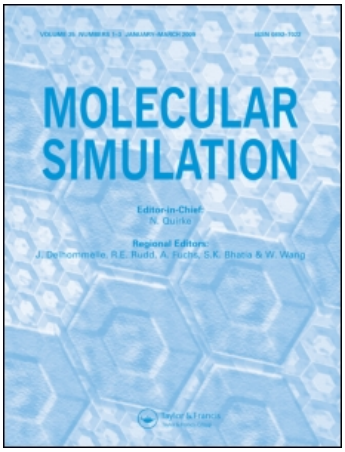

Molecular Simulation
Publication details, including instructions for authors and subscription information:
http://www.informaworld.com/smpp/title~content=t713644482

Simulated annealing effects on Na-FAU crystal reconstruction and sorption efficiency

P. Krokidas[ab]; E. D. Skouras[a]; V. Nikolakis[a]; V. N. Burganos[a]
[a] Foundation for Research and Technology Hellas, Institute of Chemical Engineering and High Temperature Chemical Processes, Patras, Greece [b] Department of Materials Science, University of Patras, Patras, Greece

To cite this Article Krokidas, P. , Skouras, E. D. , Nikolakis, V. and Burganos, V. N.(2008) 'Simulated annealing effects on Na-FAU crystal reconstruction and sorption efficiency', Molecular Simulation, 34: 10, 1299 — 1309
To link to this Article: DOI: 10.1080/08927020802208950
URL: http://dx.doi.org/10.1080/08927020802208950

Molecular Simulation
Vol. 34, Nos. 10–15, September–December 2008, 1299–1309

Taylor & Francis
Taylor & Francis Group

Simulated annealing effects on Na-FAU crystal reconstruction and sorption efficiency

P. Krokidas[ab], E.D. Skouras[a], V. Nikolakis[a] and V.N. Burganos[a]*

[a]*Foundation for Research and Technology Hellas, Institute of Chemical Engineering and High Temperature Chemical Processes, Patras, Greece;* [b]*Department of Materials Science, University of Patras, Patras, Greece*

(*Received 1 February 2008; final version received 16 May 2008*)

The accurate reconstruction of zeolite frameworks at the atomic scale is of critical importance for the study of the sorption and separation properties of these materials. In this work, the atomistic description of NaX form of the aluminosilicate faujasite (FAU) crystals is accomplished using lattice reconstruction and simulated annealing techniques. The effect of temperature on the NaX framework structure and on the precise positioning of the extra-framework cations has been thoroughly investigated using annealing cycles at several temperatures. The effects of the framework details including the cation positions on the sorption of CO_2 and N_2 in these structures are studied using molecular simulations. Comparison of simulated adsorption isotherms in non-annealed structures to experimental data reveals that the agreement is a strong function of the cation positions in the framework. More consistent results are obtained when annealing is performed, in which case the deviation in the energy calculations is reduced by almost two orders of magnitude. Cation tracking during several annealing cycles is also implemented that reveals the existence of strongly preferred positions for cations close to the Al atoms within the super cage. Comparison of the calculated and experimental values for the heat of adsorption obtained in this work reveals satisfactory agreement in both CO_2 and N_2 sorption cases for structures that have undergone simulated annealing.

Keywords: zeolites; reconstruction; sorption

1. Introduction

Nowadays, zeolites are involved in an increasingly expanding portion of science and technology, including catalytic and separation processes [1–3], gas storage [4], and ion exchange [5]. In particular, the performance of a zeolite crystal in separations (sorbents, membranes) can be described by the interplay of the mixture adsorption equilibrium and the mixture diffusion. The prediction of the sorption and separation capacity of a given zeolite membrane should be, in principle, possible on the basis of separately measured single component adsorption and diffusion data. Thus, much experimental and theoretical research effort was focused recently on zeolitic materials. This is driven not only by their technological importance but also by the fact that they provide an inherent representation of model porous systems. Zeolites are well-ordered crystalline nanoporous materials. More than 150 framework types have been identified so far making them ideal systems for the investigation of their adsorption properties against parameters such as size and shape of the pores, chemical composition of the framework (Si/Al ratio, isomorphously substituted Si by other metals, i.e. B, Fe, etc), and nature of the extra-framework cations. In the past few years, a limited number of theoretical studies have investigated the influence of either the nature or the distribution of these cations on the sorption properties of zeolite systems. Systematic studies have focused on the adsorption properties of X- and Y-faujasite systems containing various monovalent or divalent cations [5,6], with respect to different adsorbates, such as carbon dioxide, ammonia, nitrogen, argon, ethane, ethene and water vapour [7,8]. Such processes are based on specific interactions of the adsorbates with the electrostatic field induced by the cations. These investigations led to empirical relationships showing, for instance, that the heat of adsorption usually increases with increasing charge density of the cations, or with decreasing cation size. It was clearly established that the extra-framework cations play a fundamental role in the adsorption phenomena in such microporous materials.

The modelling process of the separation behaviour of a zeolite membrane is still at early stages of development. Recently, the Maxwell–Stefan model has been successfully employed for the description of the single component permeation [9] and the prediction of binary mixture permeation [10] in MFI membranes. Two transport mechanisms are assumed to overlap: surface diffusion and activated gas diffusion. Based on Molecular Dynamics (MD) and Molecular Orbital calculations it has been attempted to describe and forecast molecular permeation by computer simulation. A more detailed classification

*Corresponding author. Email: vbur@iceht.forth.gr

ISSN 0892-7022 print/ISSN 1029-0435 online

DOI: 10.1080/08927020802208950
http://www.informaworld.com

of the two-component permeation through zeolitic membranes considers (i) adsorption on the external surface, (ii) selective adsorption in the zeolite pores, and (iii) size dependent diffusivities in the zeolite pores.

Zeolite membranes can separate a mixture via a molecular sieving process, or due to large differences between the individual molecular mobilities, large differences between the adsorption potentials for each compound, or a combination of mobility and adsorption potential differences. In the case of differences in adsorption, the selectively adsorbed compound excludes the other one from entering the zeolite pores, and as a result it blocks its transmission through the membrane.

In the past, atomistic simulations of the structure of several inorganic porous materials (SiO_2, zeolites) [11–17] have been realised using MD and Monte Carlo (MC) simulations. The reconstruction of inorganic structures at the atomic scale usually includes the following conceptual steps. Initially, the atoms of the membrane material are positioned at reference bulk lattice sites using literature data. The interatomic potential energy of the configuration is dynamically calculated using a pre-selected force field description, the parameters of which have been calculated using either experimental or *ab-initio* data. Depending on the available data and the accuracy needed, simple energy descriptions, like the ones found in Universal Force Field (UFF) [18] (as well as in UFF variations), adapted to zeolite simulations [19,20] can be utilised for this purpose [21,22]. Boundary conditions are then set, either periodic or of the free surface type. The final step is the total potential energy minimisation of the system, using Steepest Descent, Conjugate Gradient and Newton–Raphson techniques, and addition of cation or other bulk/surface defects (where appropriate) in an iterative scheme. Using a force field of this kind, very useful quantities can be computed, such as momenta, interaction energies, conformational energy barriers, free energies, etc. The atomistic structure is the basis for MD and MC calculations to probe the locations, conformations, and motions of sorbate molecules, such as CO_2, and N_2, in order to draw useful conclusions concerning the actual supply of sorbates to the active sites of various types of FAU structures (DAY and NaX).

In the present work the adsorption of CO_2 and N_2 in atomistic reconstructions of the Na-FAU is studied. The interest in the particular zeolite stems from promising experimental data on their separation efficiency in the form of polycrystalline membranes [23,24]. This goal is achieved through the following procedure: An initial structure of the FAU crystal is reconstructed at the atomic level using data from the literature. However, the existing data are usually available only at room temperature, and they do not provide information about the exact position of the extra-framework cations that are present in the structure. To address these issues, a general methodology using simulated annealing is developed and used for the atomistic description of NaX FAU crystals. Adsorption isotherms are then calculated and compared with experimental results, and along with heats of adsorption, they are used for the validation of the simulation methodology proposed here. Simulated annealing is found to lower significantly the uncertainties in the prediction of sorption and separation properties of FAU.

2. Computational methodology

The faujasite unit cell having a stoichiometry close to that of experimentally investigated samples has been reconstructed using the XRD-based structural data from the work of Zhu and Seff [25]. The unit cell of NaX has cubic symmetry (Fd3m symmetry group) and its lattice constant at room temperature is 25.077 Å. The composition of the unit cell is $O_{384}Si_{100}Al_{92}Na_{92}$. Previous studies, like the one of Buttefey et al. [26], assumed that both Si and Al can be represented using a unique T atom that had the average properties of the two atoms. This assumption was introduced to sidestep the complication that would arise by the large number of possible configurations of the same crystal if Si/Al is not equal to one. If a unique T atom is not introduced, then a reliable computation of a property would require a large number of simulations in order to average over the different arrangements of Al atoms in the simulated unit cell. This number can be extremely high in the case of zeolites with high Si/Al ratio (case of NaY). On the other hand, Jaramillo and Auerbach have developed a forcefield for modeling cation motion in faujasite that explicitly distinguishes between the Si and Al atoms [27]. The minimum energy configuration of several faujasite crystals having different Si/Al ratio was obtained using a cation annealing procedure. The T-atom methodology was not used in the present work, for two reasons. First, we studied a NaX crystal of the aforementioned composition (Si/Al = 1.16), in which only four Al framework atoms have to be arranged (four degrees of freedom), thus keeping the uncertainty of the resultant configuration rather limited. Second, given that one of the goals of this study was to simulate the adsorption in NaX crystals, the clear distinction between Si and Al atoms is needed to provide a detailed simulation of the sorption process. Thus, the first step in the reconstruction is the proper placement of the Si, Al and O framework atoms, which form eight sodalite cages in FAU. Sodalite cages are interconnected with oxygen bridges forming a pore system with access window having diameter *ca*. 7.4 Å. The Si and Al atom distribution follows the Löwenstein's Al—O—Al avoidance rule [28]. The placement of the cations at specific sites is very significant also [29,30]. A view of the reconstructed unit cell of NaX, obtained with the help of Materials Studio®, is shown in Figure 1, where the red

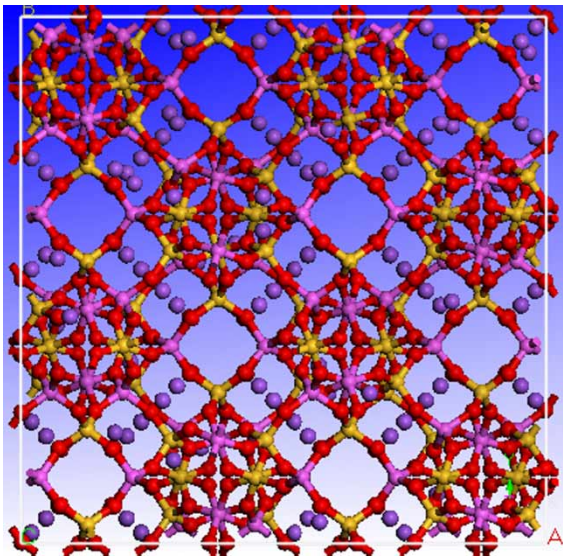

Figure 1. Unit cell of NaX faujasite.

balls represent the oxygen atoms, whereas the purple and yellow balls represent the aluminum and silicon atoms, respectively. The blue balls represent the Na cations.

The possible positions of Na^+ in the unit cell are the following: sites I located in the centre of the double six member ring connecting the sodalite cages; sites I′ located in the sodalite cage in front of the double six member ring; sites II in front of the single 6-ring window of sodalite cage; and sites III′ and III″, which are congener positions located in front of the 4-ring windows of the sodalite cages with small variations and called here sites III. Figure 2 shows a schematic representation of the Na^+ positions in the various sites, using as point of reference a sodalite cage.

The distribution of Na^+ among the different sites involved 32 Na^+ at site I′, 32 Na^+ at site II, and 28 Na^+ at site III. In the case of NaX, full occupancy of site I′ and II was assumed (32 Na^+/site). This is not the case for site III, where only 28 of the 196 symmetrical positions are occupied. This means that several alternative configurations with the Na^+ at different locations can be generated. Two possible methods were followed in order to reproduce an energy favouring structure. The first method is the one suggested in the work of Seff [25], and the second one places the Na^+ cations randomly, excluding positions that are too close to each other and, consequently, would produce unrealistic, repulsive interactions.

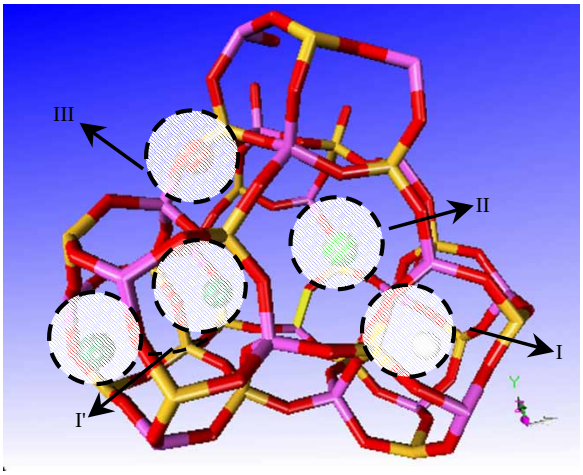

Figure 2. The possible locations of Na^+ in faujasite using the sodalite cage as a point of a reference.

2.1 *Interaction potential*

We separate the forces that act on the zeolite atoms in the presence of gas molecules into intermolecular and intramolecular ones. The intermolecular (non-bonded) interaction energy, V_n, is due to interactions among atoms of different molecules. Interactions between atoms of the same molecule or between bonded atoms are called intramolecular interactions (bonded) and correspond to the interaction energy V_b. The overall interaction energy is the sum of these two contributions:

$$V = V_b + V_n. \tag{1}$$

2.2 *Intermolecular interactions*

Intermolecular interactions are described with a Lennard-Jones potential for the Van der Waals interactions and a term for the electrostatic interactions. The general form of the relation giving the intermolecular interactions is given below:

$$V_n = V_{L-J} + V_{electrost} \quad \text{where}$$

$$\begin{cases} V_{L-J} = 4\varepsilon\left[\left(\frac{\sigma}{r}\right)^{12} - \left(\frac{\sigma}{r}\right)^{6}\right] \\ V_{electrost} = \frac{q_1 q_2}{4\pi\varepsilon r} - \frac{\mu q}{4\pi\varepsilon} \otimes \frac{1}{r^2} + \cdots \end{cases} \tag{2}$$

The interaction of the gas molecules (CO_2 and N_2) with each other and with the zeolite atoms has been described using the point charge model. In this approach every atom interacts independently of the others, and a specific charge is assigned to every atom in each gas in order to reproduce the quadruples of CO_2 and N_2. Figure 3 shows quadruples of CO_2 and N_2. An alternative approach is the united atom method, where every molecule is represented as an interaction centre, assigned a Van der Waals term and a term giving its electrostatic moment. Clearly, the former model gives a detailed and, thus, more realistic description of the way the molecules interact with each other and with the lattice atoms, provided that sufficient forcefield data for each interaction are available,

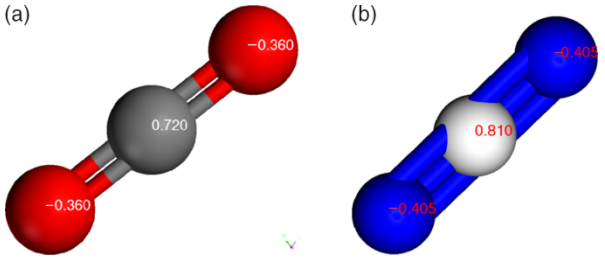

Figure 3. Representation of quadruple molecules of (a) CO_2 and (b) N_2.

which is the present case. The form of the relation for the interactions now looks simpler, since the charges of the atoms are only needed for the description of the electrostatic interactions:

$$V_n = 4\varepsilon\left[\left(\frac{\sigma}{r}\right)^{12} - \left(\frac{\sigma}{r}\right)^{6}\right] + \frac{q_1 q_2}{4\pi\varepsilon r}. \quad (3)$$

The molecules studied here are linear quadruples, so they were represented as three-point models, i.e. three points on the same line, the central atom having a specific charge and the outer ones having half the charge of the central one. Figure 3 shows the quadruples for the CO_2 and N_2 molecule.

In the case of N_2, which is a diatomic molecule, the central point is a pseudoatom which does not interact via the Van der Waals force. It serves only as a position with a specific charge that is generated in the centre of the bond between the two atoms and is responsible for the quadruple character of the molecule.

The values for the charges and the distances between the point charges forming the quadruples as well as the values for the terms of the Lennard-Jones potential used in the simulations can be found in Tables 1 and 2, respectively. The CO_2 charges were derived with the use of *ab initio* calculations, while the Lennard-Jones parameters were obtained by fitting with experimental adsorption enthalpies [31]. The charges and the diagonal Lennard–Jones parameters for the N_2 molecule are the product of a fitting procedure using experimental data of properties of the crystal structure of nitrogen at zero temperature [32]. Further details for the structure charges and potential parameters can be found in the literature [33,34].

Table 1. Charges and interatomic distances used in the simulations.

Atom	Charge	Interatomic distance (gas molecules) / Å
Si (framework)	2.4	–
Al (framework)	1.7	–
O (framework)	−1.2	–
C (in CO_2)	0.72	–
O (in CO_2)	−0.36	1.150 (C–O)
N (in N_2)	−0.483	1.098 (N–pseudo atom)
Pseudo-atom #1 (in N_2)	0.966	–

The electrostatic interactions were calculated using the Ewald summation method, and the Van der Waals terms were calculated from an atom-based summation with 12 Å cut-off distance.

2.3 *Intramolecular/bond interactions*

The motion of the Na cations in faujasite has been modeled in the past. However, in the previous studies [26,35] the movement of the framework atoms was usually ignored. Our goal was to develop a technique that can predict at different temperatures not only the cation arrangement but also the exact framework atom positioning. For this reason, a full potential model, containing interactions between both framework atoms and cation atoms was adopted.

Bonded terms in the potential expression adopted stand for forces that are generated between bonded atoms and describe the pertinent atomic motions, like oscillations and vibrations of the atoms around the equilibrium positions. These movements were used in the annealing process, where the motion of the framework as well as the vibrations of the gas molecules must be taken into account.

A theta harmonic potential was used, which describes the oscillations of the angle of the bond between Al and O atoms as well as between Si and O atoms. The theta harmonic potential has the form:

$$E = 1/2K_\theta(\theta - \theta_0)^2. \quad (4)$$

The Buckingham potential provides updated Van der Waals force terms for zeolitic atoms. The Buckingham potential is of the form

$$V(r) = A\exp(-r/\rho) - Cr^{-6}, \quad (5)$$

where ρ is a characteristic distance between the atoms (see below). While the aforementioned equation is the most commonly used, a different yet equivalent form of it was used in our calculations (Materials Studio; FORCITE, Sorption modules):

$$V(r) = D_0\left[\left(\frac{6}{\gamma-6}\right)\exp\left(\gamma\left(1-\frac{r}{R_0}\right)\right) - \left(\frac{\gamma}{\gamma-6}\right)\left(\frac{R_0}{r}\right)^6\right]. \quad (6)$$

We found the equivalent parameters for the Materials Studio description by matching the field values description of Equations (5) and (6) and solving the corresponding

Table 2. Van der Waals constants for the interaction of N_2 with the framework atoms and within the CO_2 molecule.

N_2 [32]	N	O_Z	Na^+				
ε_N(eV)	0.00314	0.0197	0.00434				
σ_N(Å)	3.318	2.708	1.746				
CO_2 [31]	O—O	C—C	O—C	C—O_z	O—O_z	C—Na	O—Na
ε_N(eV)	0.00659	0.00402	0.00158	0.00363	0.00601	0.00759	0.0027
σ_N(Å)	3.36	3.83	3.31	3.90	3.48	3.35	2.95

algebraic system (7),

$$D_0\left(\frac{6}{\gamma-6}\right)\exp(\gamma)=A,\quad \frac{\gamma}{R_0}=\frac{1}{\rho},\qquad D_0\left(\frac{\gamma}{\gamma-6}\right)R_0^6=C, \tag{7}$$

where D_0 is the bond strength or well depth of the potential in kcal/mol, R_0 is the bond length in Å, and γ is a scaling factor. The Buckingham potential does not represent a bonded potential but can be used for describing interactions between atoms belonging to a single body (zeolite).

The parameter values for these detailed potentials have been taken from the literature [20]. Coarser descriptions, like the Rigid Unit Model [35], which provide interactions between rigid groups of atoms (tetrahedra and octahedra) linked by vibrating oxygen bridges, have been used in the past for the investigation of the zeolite structure deformation, like temperature dependence of the zeolite pore dimension, and negative thermal expansion coefficients. Other methods, like the MC replica exchange method [36], predict the non-framework cation positions only, assuming that the framework atoms are fixed.

Absolute adsorption isotherms were computed using a Grand Canonical MC calculation algorithm, which allows displacements (translations and rotations), creation, and destruction, as implemented in the Sorption module of the Materials Studio software suite. These simulations consisted in evaluating the average number of adsorbate molecules whose chemical potential equals that of the bulk phase for a given fugacity (pressure) and temperature. In order to compare simulations with experimental data, the fugacity (f) and pressure (p) were related through $f = cp$, where c corresponds to the fugacity coefficient. This coefficient is known to vary with pressure and in the present work it was evaluated through an experimentally derived equation of state that accounts for gas compressibility. In fact, the gas compressibility was calculated with the aid of tables that correlate this quantity with the critical pressure and critical temperature of each sorbate. Further information on the relation among these quantities and on the origin and content of the aforementioned tables can be found in the literature [37].

All simulations were performed at 302–325 K using one unit cell of faujasite, typically allowing 6×10^6 Metropolis MC steps (for further information about the MC algorithm, the reader is referred to the related textbook of Frenkel and Smit [38]). The evolution of the total energy over the MC steps was plotted in order to control the equilibrium conditions. The zeolite structure was assumed to be rigid during the sorption process. This is a convenient yet rather reasonable assumption for the sorption process, as the heat of adsorption is primarily a function of the sorbate–framework interactions, provided that the framework is near equilibrium. However, during minimisation and simulated annealing, this assumption is removed thanks to the large flexibility in the degrees of freedom that is allowed in these cases. Cell angles and bond lengths were kept rigid at their minimum-energy locations as pinpointed by the forcefield description.

The Ewald summation was used for the calculation of the electrostatic interactions, while the short-range interactions were calculated using a cutoff distance of 12 Å. Furthermore, in order to take into consideration the steric effects that prohibit the access of N_2 and CO_2 atoms into the sodalite cages, dummy atoms with appropriate van der Waals radii were mounted into these cages. As a result, the selection of a location in the sodalite cages as an adsorption site by the MC algorithm became practically impossible. The calculations of the differential enthalpies of adsorption at zero coverage, $\Delta_{ads}h_\theta$, can be performed through the fluctuations of the number of particles in the system and through the fluctuations of the internal energy U, (i) with the consideration of very low pressures and (ii) by switching off the adsorbate–adsorbate interactions.

$$\Delta_{ads}h = RT - \frac{\langle UN\rangle - \langle U\rangle\langle N\rangle}{\langle N^2\rangle - \langle N\rangle^2}. \tag{8}$$

2.4 Simulated annealing

The annealing process consists of simulation steps that include two main parts, the first of which employs conjugate gradient and Newton-Raphson techniques for the energy minimisation of the structure at hand using a forcefield description of the interactions between atoms [39]. This part is followed by a MD simulation in an ensemble of constant number of particles, constant volume

Table 3. Parameters and results (final volume and energy of structure) for each annealing process.

	Cycles	T_{max}	Ramps	Dynam. Steps/ Ramp	Volume (Å^3)	Energy (kcal/mol × 10^{-5})
Initial	–	–	–	–	15769.8	−1.980750
1	5	533	5	40,000	15142.2	−2.011194
2	5	533	5	10,000	15149.8	−2.011126
3	5	533	5	5000	15141.35	−2.011158
4	15	533	10	50	15143.22	−2.011199

and constant temperature. At sequential steps, the temperature value is gradually increased from the initial one up to a predefined temperature limit (increasing ramp). This procedure is followed by a similar one, with gradually lower MD temperatures (decreasing ramp), down to the initial temperature. This increasing–decreasing ramp cycle is usually followed by several sequential ones to optimise results. The idea behind the simulated annealing technique is to use the MD steps and the temperature ramp to overcome local energy minima of the structure and, thus, achieve a structure configuration with a total energy minimum [38]. This would not be possible if a simple minimisation technique was used.

3. Results and discussion

As the starting point of the annealing process, the most appropriate set of numerical parameter values, including those of the number of cycles, ramps, and dynamic steps, was investigated. Initial attempts were conducted with five cycles and five ramps per annealing cycle, and the structure was allowed to move for 40,000 dynamic steps (of 1 fs) within each ramp, leading to a total of 10^6 steps. The numbers of steps and ramps were kept fixed within a simulation, the maximum temperature was set at 533 K and the initial (target) temperature was 293 K. This temperature corresponds to room conditions and is quite close to the one at which literature X-ray data were taken and used for the reconstruction of the initial structure [25]. Table 3 summarises the results of this procedure. For 5000 dynamic steps, a structure of similar energy was generated. The number of dynamic steps was gradually reduced to a number that can reproduce the equilibrium velocity distribution in the NVT ensemble at the desired temperature. A number of 50–100 dynamic steps turned out to be sufficient for the system to reach equilibrium. Thus, a number of 50 dynamic steps per ramp were used, while the number of cycles was set at 15 and the number of ramps at 10, thereby lowering the total steps to 7500. Using these optimal parameters, a crystal of the same level of energy, and of practically the same volume, was obtained, saving valuable computational time.

For validation purposes, an investigation was performed, in order to seek whether the results could indeed converge to the same structure (of minimum total energy), independently of the precise selection of the initial structure configuration. To this end, several different structures were reconstructed, using data from the work of Zhu and Seff [25]. The initial structures were divided into two groups. The first one involved unit cells in which the Na^+ cations at sites III′ and III″ were distributed using the procedure reported in Zhu and Seff [25]. In the second group, the III′/III″ site cations of the unit cell were distributed following a fully random process. The results are shown in Table 4. The number of steps that was ultimately chosen (7500) was the one which could reproduce energetically acceptable cells in the minimum simulation time without compromising noticeably the accuracy (in both geometric and energy terms) of the results. Once again, the target temperature was set at 293 K. All unit cells had an initial volume of 15,769.8 Å^3. The different distributions of Na^+ led to an energy deviation between the structures of *ca* 340 kcal/mol. On the other hand, the simulated annealing procedure, as performed on these structures, resulted in structures of lower volume by about 4%, as compared to the initial structures, and limited drastically the energy deviation down to *ca* 8 kcal/mol despite the large deviations that were noted among the initial structures.

The new positions of Na^+ at III′/III″ sites were also checked through radial distribution functions. Indeed,

Table 4. Energy and structure deviations of the various reconstructed cases (before and after simulated annealing).

	Initial volume (Å^3)	Initial energy (kcal/mol)	Energy deviation (kcal/mol)	Final volume (Å^3)	Final energy (kcal/mol)	Energy deviation (kcal/mol)
Random 1		−198074.52		15143.22	−201120	
Random 2		−197959.24		15136.45	−201103	
Random 3	15769.8	−198007.68	339.421	15139.94	−201100	7.855
Seff 1		−198638.10		15141.53	−201102	
Seff 2		−198619.64		15140.49	−201106	

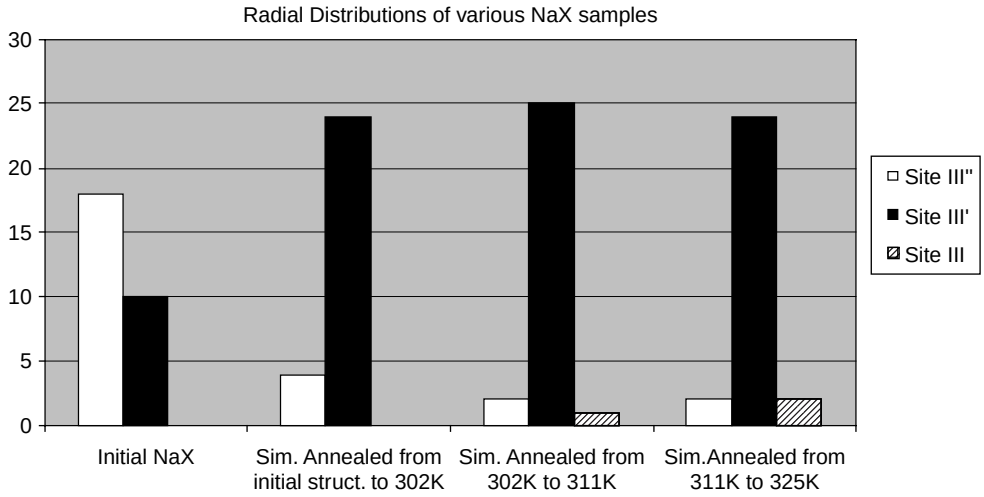

Figure 4. Occupation of sites III′, III″ and III with Na atoms positioned nearby Si and Al framework atoms (taken from radial distribution functions) in various NaX samples at 302 K: Initial NaX structure (non-annealed); NaX structure annealed at 302 K (starting from the initial structure); NaX structure annealed up to 311 K (starting from the 302 K-annealed structure); and NaX structure annealed to 325 K (starting from the 311 K-annealed structure).

while Na III′ atoms remained close to Al atoms, Na III″ atoms moved away from Si atoms and repositioned themselves in the vicinity of Al atoms. This appears to be a naturally preferable position for Na^+, since Al atoms are assigned smaller positive charges. In general, during the annealing process the only considerable transfer took place between Na^+ of III′ and III″ sites, while Na^+ at I′ and II sites remained close to their initial positions. This behavior was also evident in the radial distribution function of NaX structures that were annealed subsequently at elevated temperatures, as described in the following section.

In order to validate further the proposed modeling methodology, the sorption capacity of the reconstructing crystals was calculated and compared to experimental data both at room temperature and at higher temperatures. The simulated annealing process was expanded to higher temperatures up to 325 K. Table 5 shows the main features of the annealed unit cells at four different temperatures. The structure at each temperature was used as initial geometry in order to generate a structure at the next temperature in sequence. The reason is that it is preferable to use as initial guess a structure that corresponds to the closest possible temperature to the desirable one. Theoretically, it would be ideal to be able to allow infinitesimally small temperature steps but this would be extremely time consuming.

Table 5. Variation of the cell volume and the potential energy with the simulated annealing temperature.

Annealing temp. (K)	Cell volume (Å^3)	Energy (kcal/mol)
293	15142.09	−200440
302	15143.32	−201081
311	15142.42	−201114
325	15140.59	−201099

The significant decrease of the minimum energy uncertainty that is offered by the simulated annealing procedure renders the method very attractive for further applications, including adsorption and diffusion. However, care must be taken to allow sufficient time for equilibration at the different intermediate stages to ensure not only energy minimisation but also settling of the Na III′ and Na III″ atoms at their equilibrium positions. This can be done by studying the radial distribution of the Na III′ and Na III″ positions next to the Al and Si atoms. Figure 4 shows the Na^+ positions after annealing procedure at different temperatures. White-filled bars show Na cations that are initially next to Si atoms (site III″) and black-colored show the ones that are initially next to Al atoms (site III′). It appears that the positions next to the Al atoms (III′) are most preferred by the Na cations thanks to their weaker electrostatic repulsion by the Al atoms compared to that by the Si atoms. Jaramillo and Auerbach [27] and Olson [40] have also predicted two distinct cation positions in the $Na_{86}X$ and the $Na_{96}X$ faujasites. However, our work reveals that at elevated annealing stages, a number of cation positions equidistant to Si and Al atoms (site III, hatches) are increasingly occupied by Na atoms. The existence of such sites has also been reported by Buttefey et al. who determined the faujasite structure from X-ray diffraction data. Thus, the simulated annealing technique facilitated the overcome of energy barriers during minimisation. In fact, it is expected that the precise positioning of the Na cations will affect eventual gas loading, as will be discussed below. At this point we have to stress the fact that the proposed methodology provides a clear distinction between three

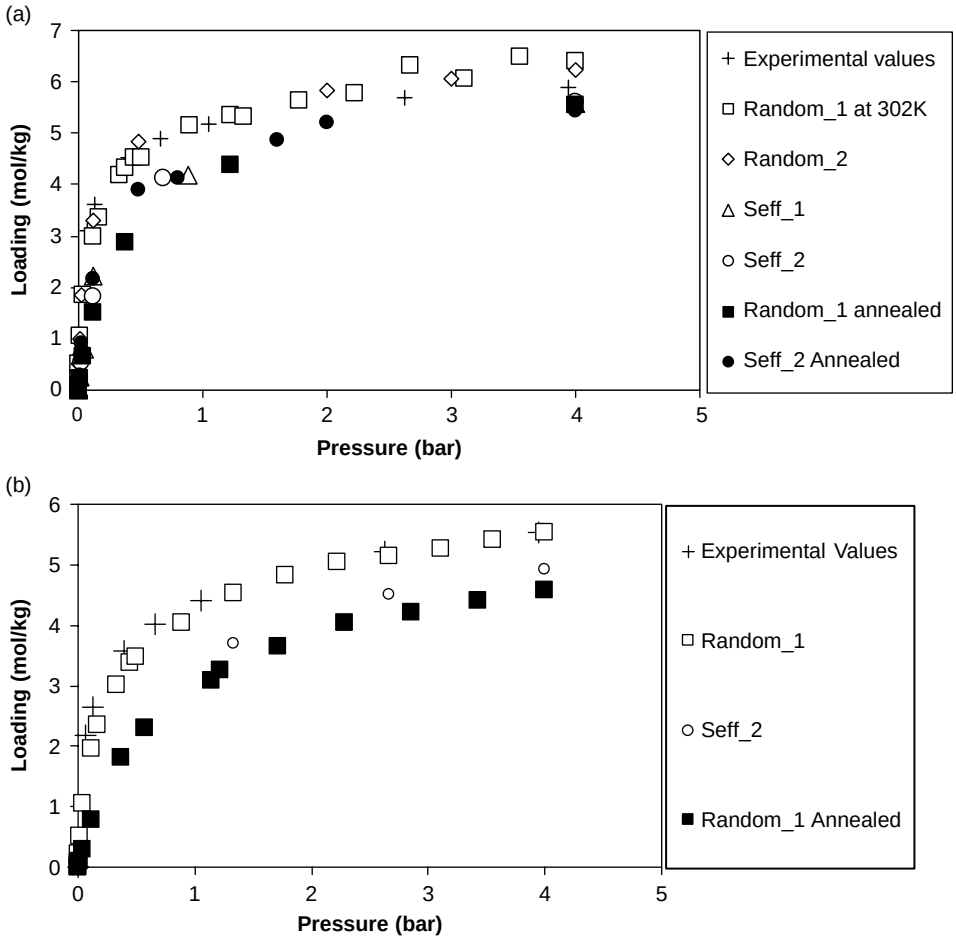

Figure 5. CO_2 adsorption isotherms in various NaX samples at (a) 302 K and (b) 325 K: Crosses represent experimental observations. Open and filled symbols correspond to non-annealed and annealed structures, respectively.

particular positions belonging to the III site family, while Buttefey et al. [26] only mention two. This differentiation is originated from the fact that Buttefey et al. used a single atom (T) to describe both Al and Si atom positions and, thus, a differentiation between III′ and III″ positions was not feasible.

3.1 Sorption results

The sorption of CO_2 and N_2 molecules was simulated at different temperatures in the initial unit cell, as well as following annealing at several temperatures. The synthesis of NaX crystals and the experimental procedure for measuring the adsorption isotherms for CO_2 and N_2 has been described in previous publications [41–44]. Calculated adsorption isotherms were compared with experimental ones. Figure 5 shows that the adsorption isotherms for non-annealed reconstructed unit cells compare satisfactorily with the experimental ones that were obtained in this work using the method described in [44] but exhibit large variations among each other especially at the elevated temperature (325 K). In fact, a small deviation between experimental and theoretical isotherms is inevitable mainly due to the large number of choices between possible cation positions (occupancies) but also due to the structural differences that are expected between the temperature of the XRD refinement and the temperature used in the calculations. Among the objectives of the annealing method is to reconstruct framework geometries that will reproduce experimental data (adsorption isotherms) with limited deviation among realisations. In this work, annealing turns out to be very efficient in reproducing satisfactory structures that lead to adsorption isotherms with notably smaller deviations, compared to those of the isotherms of structures prior to annealing. However, the deviation from experimental data increases at increased temperature. Nevertheless, this deviation is clearly smaller than the typical deviation among different sets of experimental data for the same process and the same temperature, as shown by a literature survey [45–47]. Structure annealing appears to improve the estimation of the heat of adsorption (Figure 6).

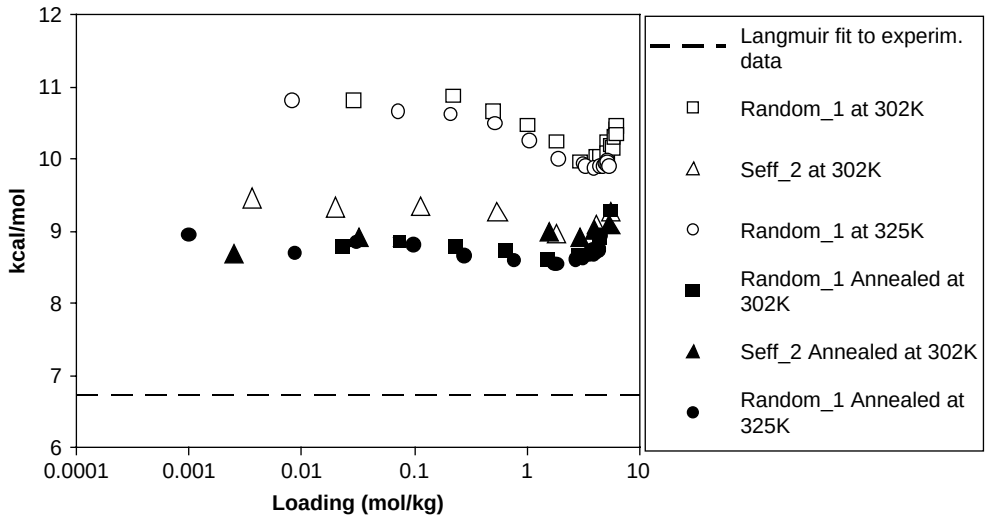

Figure 6. Heat of CO_2 adsorption. Initial NaX (non-annealed) structure for 302 K and 325 K. Open and filled symbols correspond to non-annealed and annealed structures, respectively.

A Langmuir fit to the relevant experimental data for sorption rendered a value of 6.8 kcal/mol, while the calculated values for the heat of CO_2 sorption in non-annealed and annealed structures were 10.7 and 8.7 kcal/mol, respectively.

In the case of N_2 sorption, the annealed structures provided adsorption isotherms (Figure 7) that are in very good agreement with the experimental ones and at the same time with much smaller deviation compared to that of non-annealed structures. The heat of adsorption (Figure 8) is also predicted with satisfactory accuracy considering again all factors that may have introduced some ambiguity in the precise reconstruction of the framework, as discussed above.

4. Conclusions

The atomistic reconstruction of NaX FAU crystals that was accomplished in this work revealed several interesting issues that have to be addressed in the study of adsorption in aluminosilicate zeolites. The positions of the framework atoms and of the non-framework cations have been determined at different temperatures using simulated annealing and their effect on CO_2 and N_2 sorption has been studied. More specifically, monitoring of tagged Na^+ during various annealing cycles showed that the positions close to the framework Si atoms are not favourable for Na^+, which relocate themselves to positions close to Al atoms. The present work makes a clear distinction among

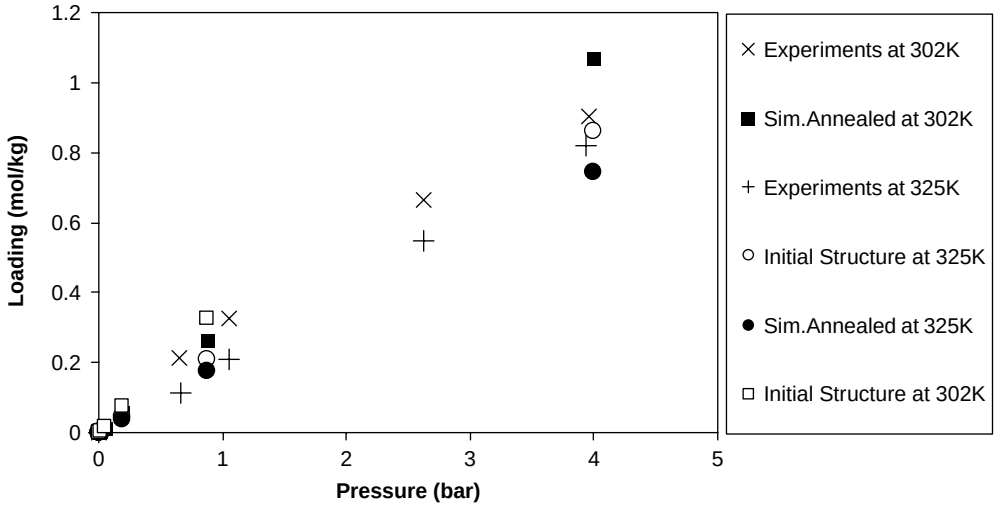

Figure 7. N_2 adsorption isotherms at 302 K and 325 K. Experimental observations [+] and [×] at 302 and 325 K, respectively. Open and filled symbols correspond to non-annealed and annealed structures, respectively.

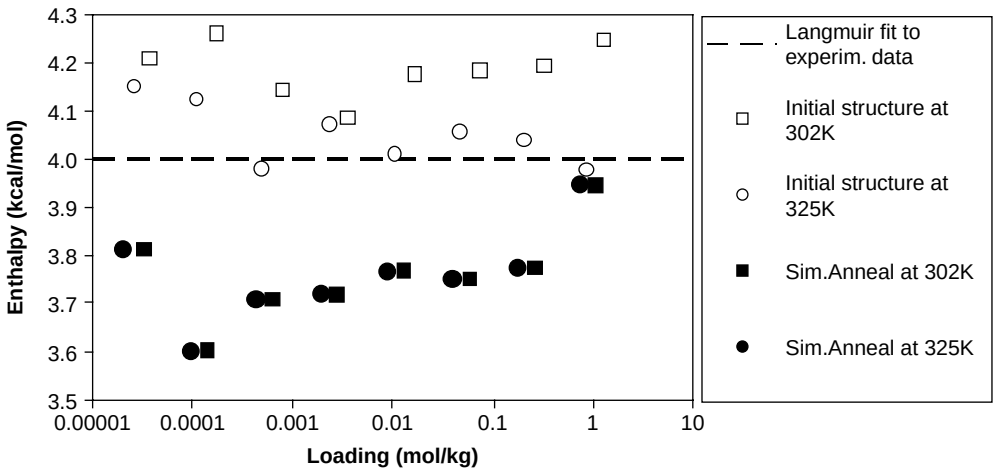

Figure 8. Heat of N_2 adsorption. Open and filled symbols correspond to non-annealed and annealed structures, respectively.

the three particular positions in the FAU cell belonging to the site III family, as dictated by recent findings, whereas simpler models in the literature only predict up to two site III variations.

Adsorption isotherms were simulated and compared to experimental data for the same conditions. It was found that the use of non-annealed and annealed structures leads to satisfactory or even excellent agreement with experiments, depending on the degree of annealing. In any case, the deviation is smaller than the deviation between different sets of experiments for the same system under the same conditions, as reported in the literature. The main benefit from the simulated annealing is that the statistical deviation in the energy calculations is reduced by almost two orders of magnitude compared to that in calculations that employed the non-annealed structure. Similar conclusions can be drawn with respect to the calculated heat of adsorption for CO_2 and N_2 in the same structures. The calculated heats of adsorption were very close to the experimental ones. It was also interesting to note a satisfactory agreement between the heats of adsorption for annealed and non-annealed structures.

In addition to MC simulation of the adsorption isotherms, MD can be used as well with the additional advantage that they can reveal accessibility effects on the loading calculation at different pressure levels, which are possibly overlooked in the standard sorption simulation. This is the subject of current work by the authors.

Acknowledgements

The authors acknowledge EU NoE NanoMemPro for financial support. We also thank Prof. M. Tsapatsis from University of Minnesota for providing access to the magnetic microbalance facility and Dr I.G. Giannakopoulos for running the adsorption measurements.

References

[1] R. Krishna and J.M. Van Baten, *Using molecular simulations for screening of zeolites for separation of CO_2/CH_4 mixtures*, Chem. Eng. J. 133 (2007), pp. 121–131.
[2] W. Jia and S. Murad, *Separation of gas mixtures using a range of zeolite membranes: A molecular-dynamics study*, J. Chem. Phys. 122 (2005), 234708.
[3] R. Krishna and R. Baur, *Modelling issues in zeolite based separation processes*, Sep. Purif. Technol. 33 (2003), pp. 213–254.
[4] H.W. Langmi, D. Book, A. Walton, S.R. Johnson, M.M. Al-Mamouri, J.D. Speight, P.P. Edwards, I.R. Harris, and P.A. Anderson, *Hydrogen storage in ion-exchanged zeolites*, J. Alloys Compd. 404 (2005), pp. 637–642.
[5] K.S. Walton, M.B. Abney, and M.D. LeVan, *CO_2 adsorption in Y and X zeolites modified by alkali metal cation exchange*, Micropor. Mesopor. Mater. 91 (2006), pp. 78–84.
[6] G. Maurin, Ph. Llewellyn, Th. Poyet, and B. Kuchta, *Influence of extra-framework cations on the adsorption properties of X-faujasite systems: Microcalorimetry and molecular simulations*, J. Phys. Chem. B 109 (2005), pp. 125–129.
[7] A.H. Fuchs and A.K. Cheetham, *Adsorption of guest molecules in zeolitic materials: Computational aspects*, J. Phys. Chem. B 105(31) (2001), pp. 7375–7383.
[8] S. Yashonath, P. Demontis, and M.L. Klein, *Temperature and concentration dependence of adsorption properties of methane in NaY: A molecular dynamics study*, J. Phys. Chem. 95 (1991), pp. 5881–5889.
[9] S. Suzuki, H. Takaba, T. Yamaguchi, and S. Nakao, *Estimation of gas permeability of a zeolite membrane, based on a molecular simulation technique and permeation model*, J. Phys. Chem. B 104 (2000), pp. 1971–1976.
[10] W.J. W. Bakker, F. Kapteijn, J. Poppe, and J.A. Moulijn, *Permeation characteristics of a metal-supported silicalite-1 zeolite membrane*, J. Mem. Sci. 117 (1996), pp. 57–78.
[11] S. Mohanty and A.V. McCormick, *Prospects for principles of size and shape selective separations using zeolites*, Chem. Eng. J. 74 (1999), pp. 1–14.
[12] V.V. Guliants, J.T. Mullhaupt, J.M. Newsam, A.M. Gorman, and C.M. Freeman, *Predicting locations of non-framework species in zeolite materials*, Catal. Today 50 (1999), pp. 661–668.
[13] H. Verweij, *Ceramic membranes: Morphology and transport*, J. Mater. Sci. 38 (2003), pp. 4677–4695.
[14] S. Murad, W. Jia, and M. Krishnamurthy, *Molecular simulations of ion exchange in NaA zeolite membranes*, Chem. Phys. Lett. 369 (2003), pp. 402–408.
[15] W. Jia and S. Murad, *Molecular dynamics simulations of gas separations using faujasite-type zeolite membranes*, J. Chem. Phys. 120 (2004), pp. 4877–4885.

[16] N. Navascués, E.D. Skouras, V. Nikolakis, N.V. Burganos, C. Tellez, and J. Coronas, *Reconstruction of umbite framework variants by atomistic simulations using XRD and sorption data*, Chem. Eng. Process 47(7) (2008), pp. 1139–1149.

[17] N. Navaschés, E.D. Skouras, V. Nikolakis, N.V. Burganos, C. Tellez, J. Coronas, and J. Santamaria, *Exploring chemical composition effects on umbite structure and gas separation properties using atomistic simulations*, Desalination 199 (2006), pp. 368–370.

[18] A.K. Rappé, C.J. Casewit, K.S. Colwell, W.A. Goddard, III, and W.M. Skiff, *UFF, a full periodic-table force-field for molecular mechanics and molecular-dynamics simulations*, J. Am. Chem. Soc. 114 (1992), pp. 10024–10035.

[19] S.L. Mayo, B.D. Olafson, and W.A. Goddard, *Dreiding: A generic force field for molecular simulations*, J. Phys. Chem. 94 (1990), pp. 8897–8909.

[20] N.A. Ramsahye and R.G. Bell, *Cation mobility and the sorption of chloroform in zeolite NaY: Molecular dynamics study*, J. Phys. Chem. B 109 (2005), pp. 4738–4747.

[21] E.D. Skouras, V. Burganos, and A.C. Payatakes, *Simulation of gas diffusion and sorption in nanoceramic semiconductors*, J. Chem. Phys. 110 (1999), pp. 9244–9253.

[22] E.D. Skouras, V. Burganos, and A.C. Payatakes, *Improved atomistic simulation of diffusion and sorption in metal oxides*, J. Chem. Phys. 114 (2001), pp. 545–552.

[23] K. Kusakabe, T. Kuroda, A. Murata, and S. Morooka, *Formation of a Y-Type zeolite membrane on a porous α-alumina tube for gas separation*, Ind. Eng. Chem. Res. 36 (1997), pp. 649–655.

[24] X. Gu, J. Dong, and T.M. Nenoff, *Synthesis of defect-free FAU-type zeolite membranes and separation for dry and moist CO_2/N_2 mixtures*, Ind. Eng. Chem. Res. 44(4) (2005), pp. 937–944.

[25] L. Zhu and K. Seff, *Reinvestigation of the crystal structure of dehydrated sodium zeolite X*, J. Phys. Chem. B 103 (1999), pp. 9512–9518.

[26] S. Buttefey, A. Boutin, C. Mellot-Draznieks, and A.H. Fuchs, *A simple model for predicting the Na^+ distribution in anhydrous NaY and NaX zeolites*, J. Phys. Chem. B 105 (2001), pp. 9569–9575.

[27] E. Jaramillo and M. Auerbach, *New forcefield for Na cations in faujasite-type zeolites*, J. Phys. Chem. B 103 (1999), pp. 9589–9594.

[28] W. Löwenstein, *The distribution of aluminum in the tetrahedra of silicates and aluminates*, Am. Mineral. 39 (1954), pp. 92–96.

[29] P. Krokidas, E.D. Skouras, V. Nikolakis, and V.N. Burganos, *Molecular simulation of sorption and separation in hydrated and non hydrated zeolites*, Proc. 3rd Panhellenic Symp. Porous Mater. (2007).

[30] P. Krokidas, E.D. Skouras, V. Nikolakis, and V.N. Burganos, *Investigation of gas sorption and separation in zeolites using molecular simulation techniques*, 4th Int. Zeolite Membr. Meeting, Zaragoza, Spain, 2007.

[31] D.F. Plant, G. Maurin, H. Jobic, and P.L. Llewellyn, *Molecular dynamics simulation of the cation motion upon adsorption of CO_2 in faujasite zeolite systems*, J. Phys. Chem. B 110(29) (2005), pp. 14372–14378.

[32] C.S. Murthy, K. Singer, M.L. Klein, and I.R. McDonald, *Pairwise additive potentials for nitrogen*, Mol. Phys. 41(6) (1980), pp. 1387–1399.

[33] E.D. Akten, R. Siriwardane, and D.S. Sholl, *Monte Carlo simulation of single- and binary-component adsorption of CO_2, N_2, and H_2 in zeolite Na-4A*, Energy Fuel 17(4) (2003), pp. 977–983.

[34] G. Maurin, R.G. Bell, S. Devautour, F. Henn, and J.C. Giuntini, *Modelling the effect of hydration in zeolite Na^+ -Mordenite*, J. Phys. Chem. B 108 (2004), pp. 3739–3745.

[35] A.P. Giddy, M.T. Dove, G.S. Pawley, and V. Heine, *The determination of rigid-unit modes as potential soft modes for displacive phase transitions in framework crystal structures*, Acta Cryst. A49 (1993), pp. 697–703.

[36] C. Beauvais, X. Guerrault, F.X. Coudert, A. Boutin, and A.H. Fuchs, *Distribution of sodium cations in faujasite-type zeolite: A canonical parallel tempering simulation study*, J. Phys. Chem. B 108(1) (2004), pp. 399–404.

[37] J.M. Smith and H.C. Van Ness, *Introduction to chemical engineering thermodynamics*, McGraw-Hill Chemical Engineering Series, New York, 1987.

[38] D. Frenkel and B. Smit, *Understanding Molecular Simulation: From Algorithms to Applications*, Academic Press, New York, 2002.

[39] M.W. Deem and J.M. Newsam, *Framework crystal structure solution by simulated annealing: Test application to known zeolite structures*, J. Am. Chem. Soc. 114 (1992), pp. 7189–7198.

[40] D.H. Olson, *The crystal structure of dehydrated NaX*, Zeolites 15 (1995), pp. 439–443.

[41] S. Qiu, J. Yu, G. Zhu, O. Terasaki, Y. Nozue, W. Pang, and R. Xu, *Strategies for the synthesis of large zeolite single crystals*, Micropor. Mesopor. Mater. 21 (1998), pp. 245–251.

[42] V. Nikolakis, G. Xomeritakis, A. Abibi, M. Dickson, M. Tsapatsis, and D.G. Vlachos, *Growth of a faujasite-type zeolite membrane and its application in the separation of saturated/unsaturated hydrocarbon mixtures*, J. Membr. Sci. 184(2) (2001), pp. 209–219.

[43] I.G. Giannakopoulos, K. Kalabaliki, V. Drakopoulos, and V. Nikolakis, *Synthesis of faujasite membranes for the separation of propane/propylene mixtures*, Stud. Surf. Sci. Catal. 158(1) (2005), pp. 137–144.

[44] T. Baimpos, I.G. Giannakopoulos, V. Nikolakis, and D. Kouzoudis, *Effect of gas adsorption on the elastic properties of faujasite films measured using magnetoelastic sensors*, Chem. Mater. 20 (2008), pp. 1470–1475.

[45] J.S. Lee, J.H. Kim, J.T. Kim, J.K. Suh, J.M. Lee, and C.H. Lee, *Adsorption equilibria of CO_2 on zeolite 13X and zeolite X/activated carbon composite*, J.Chem. Eng. Data 47 (2002), pp. 1237–1242.

[46] J.A. Dunne, M. Rao, S. Sircar, R.J. Gorte, and A.L. Myers, *Calorimetric heats of adsorption and adsorption isotherms. 2. O_2, N_2, Ar, CO_2, CH_4, C_2H_6, and SF_6 on NaX, H-ZSM-5, and Na-ZSM-5 zeolites*, Langmuir 12 (1996), pp. 5896–5904.

[47] S. Cavenati, C.A. Grande, and A.E. Rodrigues, *Adsorption equilibrium of methane, carbon dioxide, and nitrogen on zeolite 13X at high pressures*, J. Chem. Eng. Data 49 (2004), pp. 1095–1101.